Research Square

Preprints are preliminary reports that have not undergone peer review.
They should not be considered conclusive, used to inform clinical practice,
or referenced by the media as validated information.

Responses of Soil Water Potential and Plant Physiological Status to Pulsed Rainfall Events in Arid Northwestern China: Implications to Disclose the Water-use Strategies of Desert Plants

Yuanyuan Ma
Northwest Institute of Eco-Environment and Resources
Hu Liu (lhayz@lzb.ac.cn)
Northwest Institute of Eco-Environment and Resources https://orcid.org/0000-0003-4263-7926
Wenzhi Zhao
Northwest Institute of Eco-Environment and Resources
Li Guo
Penn State Department of Ecosystem Science and Management: The Pennsylvania State University Department of Ecosystem Science and Management
Qiyue Yang
Northwest Institute of Eco-Environment and Resources
Yulong Li
Hebei Key Laboratory of Geological Resources and Environment Monitoring and Protection
Jintao Liu
Hohai University State Key Laboratory of Hydrology Water Resources and Hydraulic Engineering
Omer Yetemen
Eurasia Institute of Earth Sciences, Istanbul Technical University

Research Article

Keywords: Water use efficiency, Manipulation experiments, Desert environments, Haloxylon ammodendron

Posted Date: October 9th, 2023

DOI: https://doi.org/10.21203/rs.3.rs-3354801/v1

License: This work is licensed under a Creative Commons Attribution 4.0 International License. Read Full License

Abstract

Soil water potential (SWP) is vital for plant productivity and ecosystem functioning. This is especially true in arid regions, where rainfall typically falls in brief pulses of variable size. This work aims to improve understanding of the response of SWP to varied rainfall pulses, and of the water-use strategies of a typical desert plant (*Haloxylon ammodendron*, HA) in arid northwestern China. Rainfall manipulation experiments and field measurements were conducted on HA to explore the response features of SWP and plant physiological status to pulsed rainfall events of varied magnitudes and durations. Multivariate Adaptive Regression Splines (MARS) was used to rank the factors influencing the response patterns of these variables. The response rate and amplitude of SWP increased with rainfall magnitude, and was most affected by three vital factors (antecedent SWP, rainfall amplitude, and rainfall intensity). Very small rainfall (< 2 mm) can increase SWP in the 20-cm layer by nearly 30%, and thus is likely to contribute to the drought relief of HA under low antecedent SWP (< -3.5 MPa), while large rainfall events (> 15 mm) influence deep SWP (60 cm) and enhance the positive correlation between SWP and soil temperature. Very small events play a vital role in maintaining SWP and promoting water use of desert plants. With longer intervals between future rainfall events, HA will tend to improve its water utilization efficiency. Given the nature of plants' utilization of small rainfall events, re-examining ecologically valid SWP thresholds of HA and other similar desert plants is critical.

1. Introduction

Drylands represent vulnerable areas of the terrestrial environment and are extremely sensitive to climate change, due to longer dry spells, lower water availability, and severe ecological degradation (Chen et al., 2016; Prăvălie, 2016; Schimel, 2010). Precipitation events in drylands are characterized by brief pulses of varying amounts, short durations (minutes or hours), and unpredictable intervals of drought (Noy-Meir, 1973). This infrequent, discrete and largely unpredictable water input has been widely regarded as a vital driver of dryland hydrological and biological processes, influencing vegetation distribution, metabolic activities, the nitrogen-carbon-water cycle, etc. (Collins et al., 2014; Noy-Meir, 1973). Short periods of resource fluctuations triggered by these rainfall pulses can satisfy the resource requirements of some biological processes over time and are sufficient to allow certain species to survive, even those on the verge of extinction (Schwinning and Sala, 2004). Many works have highlighted a series of responses caused by different rainfall pulse sizes. Small rainfall events (< 5 mm), for example, may only stimulate the activity of soil microorganisms (Cui and Caldwell, 1997), whereas large events (> 25 mm) can trigger the germination of many desert plants and increase the rate of carbon fixation (Schwinning and Sala, 2004; Schwinning et al., 2003). Therefore, these discrete rainfall pulses play an important role in maintaining the physiological activities of plants and regulating the water-carbon balance in arid ecosystems by triggering ecosystem cascade reactions (Goodwell et al., 2018; Huxman et al., 2004). Exploring the variability and hierarchy of eco-hydrological responses to pulsed rainfall events is of crucial importance for understanding dryland issues, including water shortages, ecological degradation, and biodiversity decrease, especially in the context of climate change and rapid urbanization (Rodriguez-Iturbe, 2000).

Many paradigms have been adopted for understanding the response of water-limited environments to rainfall pulses, such as the pulse-reserve paradigm (Noy-Meir, 1973; Reynolds et al., 2004), which considers water as a primary variable organizing biological responses and organismal adaptation through effects on energy and carbon storage (Reynolds et al., 2004; Yang et al., 2008). Related concepts and methods have been developed to describe the functional response of ecosystems to rainfall or soil moisture pulses, such as the threshold-delay model proposed by Ogle and Reynolds (2004), the “pulse dynamic” framework expanded from the pulse-reserve paradigm by Collins et al. (2014), and dynamic process connectivity, introduced by Goodwell et al. (2018). These studies emphasized that intermittent variability of resource inputs and the non-linear responses of plants or soil microbes to inter- and intra-annual variations in rainfall affect both the magnitude and the temporal dynamic of ecosystem responses to rainfall (Potts et al., 2006). However, the effects of pulsed environmental flow (rainfall pulses in particular) on vegetation physiology and ecology are still controversial. For example, many researchers have suggested that a rainfall event of over 5 mm is generally considered to be ecologically significant,

while others have stressed that the threshold of rainfall should be a dynamic variable, following the growth patterns of plants (Hao et al., 2012; Sala and Lauenroth, 1982). Rainfall is the main source of soil water for drylands, as it changes the soil water state and provides the necessary resources for the survival of plants (Petrie et al., 2015; Sala and Lauenroth, 1982). Soil water status is important in regulating photosynthesis and controlling land surface-climate feedbacks at both the local and global scales. Since the response of soil water to rainfall produces a series of ecological effects, evaluating the response of soil water status under the influence of rainfall pulse is crucial for understanding vegetation growth and maintenance in xeric areas.

Soil water status is characterized by both the amount of water present (soil water content, SWC) and the energy with which the water is held (soil water potential, SWP) (Papendick and Campbell, 1981; Passioura, 1982). SWP describes the energy state and movement characteristics of water in the soil, providing information on the availability of water for plant absorption or microbial activity, as well as whether and how the soil retains or releases water in the soil-plant-atmosphere continuum (SPAC) (Luo et al., 2022; McKenzie et al., 2002; Novick et al., 2022). Accordingly, SWP is the result of inherent properties of soil water itself, and of its physical and chemical interactions with its surroundings. SWP is a robust descriptor of the soil water regime and an important index to measure the effectiveness of soil water for plant utilization (Huber et al., 2014; Luo et al., 2022; Novick et al., 2022). Indeed, the dynamic feature of SWP is also vital for plant productivity and ecosystem functioning (Dasgupta et al., 2015; Nolz et al., 2013). For example, fluctuations in SWP caused by pulsed rainfall determine the availability of soil water to plants, controlling plant germination, and regulating plant transpiration, as well as affecting the participation of microbial activity in soil organic matter transformation, thereby helping plants access limited resources (Polley et al., 2016; Schwinning and Sala, 2004). Understanding the response of SWP to varied rainfall pulses provides vital insights into the ecological impacts and plant adaptations to climate change and rainfall variability, and thus helps us better manage drylands in a sustainable way (Grunzweig et al., 2022; Hudson, 2019; Long et al., 2021). However, few works so far have investigated this issue.

Haloxylon ammodendron (HA) is one of the main constructive perennial species widely distributed in northwestern China and in many other arid regions of the Asian and African continents (Gao et al., 2020; Zheng and Wang, 2014). Because of its remarkable tolerance to drought and great ability to survive in harsh environments, HA is also often adopted in the afforestation of arid areas around the world, as a way of combating desertification (Zou et al., 2010). HA responds to rainfall pulses and manages water use via its unique root system. When water is abundant, HA's fine roots, which are dispersed over the upper soil layer and have significant ecological plasticity, can access shallow water; and the vertically growing and well-developed taproot system can access deep water over a broader area when the surface water supply is insufficient. According to the majority of studies, HA responds considerably to rainfall pulses larger than 5 mm and primarily utilizes shallow soil water to support its life activities (Zou et al., 2009). Rainfall of less than 5 mm is typically regarded as ineffective, although some researchers point out that a minor 1-mm rainfall event can change HA's stomatal behavior directly or indirectly (Yu et al., 2013). In fact, the water-use strategies of HA remain inadequately investigated, especially its role of utilizing small rainfall pulses (i.e., < 5 mm) (Dawson and Pate, 1996; Zou et al., 2009). In this study, therefore, rainfall manipulation experiments and field observations were carried out on HA in the arid desert area of northwest China, to determine the characteristics of SWP and how plant physiological status is affected by various rainfall pulses. We hypothesized that 1) Small rainfall pulses (< 5 mm) are crucial for the physiological activities of HA, maintaining the physiological activities of plants stimulated after heavy precipitation events and improving water use efficiency. 2) The use efficiency of HA to small rainfall events increases with the increase of rainfall intervals or dry periods, thus promoting the survival of HA in harsh (low-SWP) environments.

2. Materials and Methods

2.1 Experimental site and plant species

The climate in this region is arid and semi-arid, with the rainy season mainly concentrated in summer. Annual precipitation and spatial distribution vary greatly, with an average of 116.8 mm/year. Precipitation below 5 mm accounts for 44.07% of the total precipitation amount and 86% of the total events. The annual average temperature is 7.6 ℃, and the potential evaporation is 2390 mm/y, 20 times the precipitation amount (Zhao and Liu, 2010). The annual relative humidity is about 46% (Zhao et al., 2009). The main soil types are sandy or sandy loam and the soil texture in this region is relatively coarse, in which 0.25 – 0.05 mm particles account for 80%-90%, the organic matter content makes up 0.12%-0.83%, and the soluble salt content is less than 0.1% (Zheng and Wang, 2015). The groundwater table is relatively deep (7 m on average) and fluctuates seasonally with an average range of 0.9 m. Vegetation in this region is dominated by xerophytic, super-xerophytic and salt-tolerant plants, most of them annual and perennial plants, such as *Haloxylon ammodendron* (HA), *Reaumuria soongorica*, *Nitraria tangutorum*, *Calligonum mongolicum*, and *Sympegma regelii*. Among the local plants, HA is one of the most typical C_4 species inhabiting the desert environments of the study area, such as piedmont alluvial fans, siltation plains, saline-alkali land, or fixed sand dunes (Liu et al., 2020). The cortex of annual shoots and succulent shoots plays major roles in photosynthesis and carbon assimilation, respectively, which can enable HA to reduce the photosensitive area and water loss from the plant. Because of its ability to reduce wind and sand erosion, this species has critical ecological and economic value, and is a suitable plant for the restoration of degraded arid regions (Shan et al., 2009).

2.2 Experiment Design and Field Measurements

A three-year field experiment (May to October, 2016–2018) was carried out at the Linze Station (a field station of Chinese National Ecosystems Observation and Research Network) in northwest China (39°19'-39°21'N, 100°02'-100°21'E) (Fig. S1ab). Seven individual HA of average age (about 10 years) and size (about 2.0 m in height) were selected to set up the experiment, which consisted of six treatments (-10%, -20%, -30%, + 10%, + 20%, and + 30%) and a control group (CK) (margin of error was ± 0.3%) with no obvious signs of past disturbance (Fig. S1c) (Liu et al., 2020; Yang et al., 2014a). The makeshift rainfall intercept-guide devices used to conduct the experiments were 2 × 2 × 2 m in size and composed of steel frames, shelter roofs, and rainfall-intercept guide pipes (Fig. S1d). The shelter roofs covered V-shaped UV-transparent polyethylene sheets (WATU, China) and were arranged in a density calculated to reduce each rainfall event by 10%, 20%, and 30% (corresponding to the treatments of -10%, -20%, and − 30%, respectively). The reduced rainfall water was collected through a gutter connected to a funnel and a rainfall-intercept guide pipe that directed water away from the reducing plots to water-addition plots (corresponding to the treatments of + 10%, + 20%, and + 30%, respectively). There were regularly spaced holes under the side-by-side pipes, which could release the rainwater collected by the shelter roofs into the water-addition plots. To prevent the blockage of the pipes by wind-blown sand, a gauze net was installed on the funnel where the water entered the pipe, for protection.

The SWP and soil temperature were measured as 10-min-mean data using sensors MPS-2 (Decagon Devices, Pullman, WA, USA), which were horizontally installed at five different depths below the soil surface (20 cm, 40 cm, 60 cm, 80 cm, and 100 cm) at each plot according to the root distribution characteristics of HA (the absorbing roots of HA are mainly distributed at the depth of 0.1-1 m soil layers). Consecutive readings at 10-minute intervals were logged with an EM50 data logger (Decagon Devices, Pullman, WA, USA). To reduce the variations in the soil profile and soil structure, the soil was excavated vertically layer by layer. After all the sensors were installed, the soil excavated in each layer was replaced separately, and then backfilled in sequence. Physiological (photosynthetic rate, P_r; stomatal conductance, g_s; transpiration rate, T_r) and morphological (leaf area) indicators of the HA under six rainfall treatments and a control group were measured by a portable photosynthesis system (LI-6400XT, Li-COR Inc., Lincoln, NE, USA) and leaf area meter (LI-3000, LI-COR, Inc., Lincoln, NE, USA) from 10 a.m. to 11 a.m. the day before and after rainfall events of different sizes during study period from July to August (2016–2018). At least three replicates were selected for each treatment and the average value calculated. For specific measurement steps, refer to Li-Cor (2011). The tap root depth of HA was determined by digging the soil profile after the study, when the groundwater level was rather high, and was found to be, on average, 4.5 m deep and well above the groundwater level (approximately 6.5 m). Plant water use efficiency (WUE) was calculated on the leaf scale by using net photosynthetic rate (A_n) and transpiration rate (T_r): $WUE = A_n/T_r$. The meteorological variables, including hourly precipitation,

relative humidity, temperature, net and global radiation, and wind velocity, were automatically recorded by an AG1000 automatic weather station (Onset Computer Corporation, Pocasset, MA, USA) located at the Linze Inland River Basin Comprehensive Research Station.

2.3 Data Analysis

We selected a study period from 2016 to 2018 (May 1 to October 31 of each year) (Fig. 1). The measured series was divided into 86 independent rainfall events based on the minimum time between events criterion: that is, the minimum time interval between two rainfall events (interval without rainfall) was longer than 6 hours (David et al., 2006; Dunkerley, 2008; Lozano-Parra et al., 2016). According to previous studies in our research area, from 1965 to 2013, individual rainfall amounts of 0–5 mm, 5–10 mm, 10–15 mm, 15–20 mm, and > 20 mm occupied 44.07%, 24.83%, 16.08%, 5.32%, and 9.70% of total annual rainfall in the study region, respectively (Yang et al., 2014a). Based on the characteristics of rainfall in the past and the pattern of plant physiological responses to rainfall events, we divided these 86 rainfall events into 6 groups (G1-G6): 0–2 mm, 2–5 mm, 5–10 mm, 10–15 mm, 15–20 mm, and 20–30 mm (Table 1), which correspond to the classification standards of Yang et al. (2014a) for rainfall. In order to assess the characteristics of rainfall pulses, we calculated intensity-duration-frequency (IDF) curves using data from 2009 to 2018, which describe the relationships among rainfall intensities, duration, and occurrence probability or average return period (Chow, 1953; Fauer et al., 2021). More details about creating IDF curves can be seen in Fauer et al. (2021) and Ulrich et al. (2020).

Table 1
Characteristics of rainfall event indices for the different groups (mean ± SD)

Group	Tot. rainfall (mm)	Avg. duration (hour)	Avg. intensity (mm/hour)	Max. intensity (mm/hour)	Avg. time to max. intensity (hour)	Avg. amount to max. intensity (mm)	Avg. intensity to max. intensity (mm/hour)	Avg. no rainfall period (hour)	Avg. antecedent rainfall indices (mm)
G1	48.00	3.10 ± 3.04	0.38 ± 0.35	1.60	1.74 ± 1.70	0.62 ± 0.44	0.43 ± 0.29	161.74 ± 174.07	30.38 ± 39.08
G2	50.60	6.67 ± 3.75	0.69 ± 0.40	3.40	3.20 ± 2.48	2.53 ± 0.76	1.24 ± 0.86	104.80 ± 120.33	39.29 ± 31.59
G3	43.20	6.33 ± 3.73	1.54 ± 0.75	5.20	2.17 ± 1.34	4.23 ± 1.53	2.66 ± 1.42	117.17 ± 139.38	53.70 ± 27.41
G4	11.80	37.00	0.32	1.80	30.00	10.80	0.36	10.00	36.00
G5	20.80	22.00	0.95	4.20	20.00	20.60	1.03	21.00	45.00
G6	55.00	25.50 ± 12.50	1.44 ± 0.73	7.20	5.50 ± 2.50	13.70 ± 9.30	2.17 ± 0.70	174.50 ± 143.50	20.10 ± 12.70

Rainfall indices for event characteristics included total amount, duration, maximum and average intensity, time to maximum intensity and average intensity from the start to the time of maximum intensity, and antecedent rainfall indices per rainfall event (Graham and Lin, 2011). We collected SWP and soil temperature data for the different treatments (-10%, -20%, -30%, CK, + 10%, + 20%, and + 30%) (-30% data for 2018 is missing) and depths (20 cm, 40 cm, 60 cm, 80 cm, and 100 cm). To normalize for the temperature sensitivity of the MPS-2 sensors, data calibration was performed in postprocessing (Walthert and Schleppi, 2018). We calculated the variation of SWP and soil temperature to compensate for temperature effects according to Walthert and Schleppi (2018).

The absolute change value of SWP ($\Delta\psi$, ψ_{max}- ψ_{min}), the interval between the arrival time of maximum rainfall intensity and the peak arrival time of the SWP response (T_{p-p}), and the time of the SWP response (T_m, the time for SWP to rise from

minimum to maximum) were chosen as the three main variables to measure the response of SWP to rainfall (Fig. 2).

SWP and soil temperature indices included antecedent SWP (soil water potential value one hour before rainfall), amplitude of SWP (*Ap*), SWP change rate (*Vswp*), the maximum hourly rate of change of SWP (Max. h. *Vswp*), and the average hourly rate of change in soil temperature (Avg. Stv). The SWP amplitude (*Ap*) and the SWP change rate (*Vswp*) can be calculated by

$$Ap = \frac{(\psi_{min} - \psi_{max})}{\psi_{min}} \times 100 \#\,(1)$$

$$Vswp = \frac{\Delta\psi}{T} \times 100 \#\,(2)$$

where ψ_{min} and ψ_{max} are the minimum and maximum values of SWP after rainfall began, respectively, and T is the time that it takes for the SWP to change.

We used Multivariate Adaptive Regression Splines (MARS) to analyze the factors affecting SWP responses. This is a non-parametric regression method of machine learning, which is suitable for simulating the interaction between a response and its influencing factors (Friedman, 1991). MARS divides a data set into segments and models them separately, generating piecewise curves known as basic functions, which can be expressed as

$$\max(0, x - t) = \begin{cases} x - t, \text{if} x \geq t \\ 0, \text{ otherwise} \end{cases} \#\,(3)$$

where x is the input variable and t is the value at which a knot is defined.

The MARS model consists of pairs of basic functions (BFs) interacting with each other:

$$f(X) = \gamma_0 + \sum_{n=1}^{N} \gamma_n \eta_n (X) \#\,(4)$$

where η_n is a basic function, the γ term is a constant coefficient and n is the number of segments (Deo et al., 2017; Friedman, 1991; Singh et al., 2021). MARS was used to rank the factors of the response of impression to SWP based on the number of times a variable was used in modeling η_n ($N_{subsets}$) and the residual sum of squares (RSS).

The coefficient of determination (R^2) and root mean squared error (RMSE) were used to evaluate the accuracy of the developed model:

$$R^2 = 1 - \frac{\sum_{i=1}^{n} \left(Y_i - \bar{Y}\right)^2}{\sum_{i=1}^{n} \left(y_i - \bar{y}\right)^2} \#\,(5)$$

$$RMSE = \sqrt{\frac{1}{n} \sum_{i=1}^{n} (Y_i - y_i)^2} \#\,(6)$$

where Y_i, $\bar{Y}$, $\bar{y}$ and n are the observed response variable, the predicated response variable, the mean of the observed response variable, and the number of SWP measurements used in the analysis, respectively.

All analyses of the rainfall and SWP data were conducted using the R software (version 4.1.0; R Studio, Inc.), with the level of significance for all statistical tests set at $P < .05$. The statistical significance of independent variables and their potential relationships with response variables and regression coefficients were tested using ANOVA, focusing on SWP and its influencing factors. The Pearson's correlation coefficient (r) was used to test the correlations among SWP, soil temperature, and meteorological factors.

3. Results

3.1 Characteristics of Pulsed Rainfall Events

A total of 86 rainfall events were delineated during the study period (May to October, 2016–2018), with a total rainfall of 229.40 mm, which accounted for 85.41% of the total rainfall over these three years, and the monthly average rainfall was highest in August (32.87 ± 12.08 mm) (mean ± SD) (Table 2, Fig. 3a). The research period was relatively dry, as seen by the average annual rainfall (76.47 ± 19.20 mm), being less than the multi-year (almost 10 years) average (90.82 ± 15.14 mm) (Fig. 3b). According to the IDF curves, taking 2-year (once in 2 years) curve and 100-year (once in 100 years) curve as examples, the area between the two lines is a high-intensity rainfall region (Fig. 3c). Only the rainfall intensity in 2018 was relatively high. The rainfall intensity in 2017 was close to the once-every-two-year curve when it persisted for more than 16 hours. In general, there was less high-intensity rainfall in 2016 and 2017. Among the six groups, Group 1 (0–2 mm) experienced the largest number of rainfall events and the number of small rainfall events (< 5 mm) accounted for 88.37% of the total number of rainfall events. In addition, there was great variability in duration (from 0.1 to 38 h) and the maximum rainfall intensity (from 0.2 to 7.2 mm/h). The period of no rainfall in the previous period ranged from 7 hours to more than 30 days. Both the timing of the rainfall and the variation of the no-rainfall period before an event revealed the discontinuity and unpredictability of rainfall pulse events. Thus, it can be concluded that the rainfall events accorded with the characteristics of pulsed rainfall.

Table 2
Characteristics of the rainfall events during the growing seasons of 2016 to 2018

Year	Number of rainfall events	Total rainfall (mm)	Mean rainfall intensity (mm/day)	Mean rainfall event size (mm)	Maximum rainfall event size (mm)
2016	29	57.00	0.50 ± 0.54	1.97 ± 2.47	11.80
2017	27	102.60	6.33 ± 7.80	3.8 ± 6.07	26.80
2018	30	69.80	2.91 ± 3.78	2.33 ± 5.19	28.20

3.2 Dynamic Features of SWP in Time and Profiles

Seasonal fluctuations are clearly present in SWP. Early in May, there was little rainfall and a low SWP value. The average SWP under different rainfall treatments was − 3.14 ± 3.81 MPa, with the average SWP under the + 20% treatment being the highest (-2.63 ± 2.03 MPa). The lowest mean value (-3.69 ± 5.84 MPa) was found under the − 10% treatment. In June, the SWP fluctuations in the shallow soil layers (20–40 cm) showed a unique “sawtooth” shape (Fig. S2), due to the lower amounts of, and more scattered, rainfall. The average SWP was 1.33 ± 3.36 MPa higher than that in May. The peak value of SWP (-0.01~-0.0001 MPa) was mainly concentrated in August, and the average SWP under different treatments was − 1.55 ± 0.66 MPa, among which the average SWP under the + 30% treatment was the maximum (-1.37 ± 0.54 MPa). SWP dropped to pre-rainy or even lower levels in October.

The vertical profiles of SWP under different rainfall treatments were similar, showing an “S-shaped” curve (Fig. 4). Except for the surface layer (20 cm), the average SWP in each layer was between − 5.5 and − 2.0 MPa. The average SWP in the shallow layers (20–40 cm) (-11.03 ± 7.25 MPa) was always higher than that in the deep layers (60–100 cm) (-2.86 ± 1.48 MPa), and more interestingly, the average SWP in the 40-cm layer was higher than that in the 20-cm layer, and the difference between the two was about 10 MPa. The average SWP was highest in the 60-cm layer (-2.42 ± 0.56 MPa). The SWP in the 80-cm layer was lower; the mean value was − 3.16 ± 2.39 MPa. The SWP of this layer fluctuated obviously only under the treatment of -20% rainfall in 2017 (Fig. S2). The average SWP at 100-cm depth (-3.00 ± 1.23 MPa) was higher than that at 80-cm depth; it may have been affected by root distribution, plant water use, and soil texture.

3.3 SWP Responses to Pulsed Rainfall Events

We divided the rainfall events into two groups: events with rainfall in the first 48 hours (R) and events with no rainfall for 168 hours (NR). Each group was divided into three classes according to rainfall levels (0–5 mm, 5–15 mm, and 15–30 mm), and

analyzed with three indices ($\Delta\psi$, T_{p-p}, and T_m) of SWP response characteristics (Fig. 5). The change value of SWP ($\Delta\psi$) for the 20- and 60-cm depths under large events (> 15 mm) and + 30% treatment was more than twice that under the − 30% treatment. The maximum $\Delta\psi$ reached 4.5 MPa when responding to large events without antecedent rainfall under + 30% treatments, while small rainfall events (< 5 mm) could cause an average change of $\Delta\psi$ in the surface layer (20 cm) of more than 2 MPa under all treatments. The arrival time of peak rainfall intensity and peak SWP response (T_{p-p}) varied between rainfall event sizes and ranges, from − 13 to 83 h (Fig. S3). Negative values of T_{p-p} indicate that the maximum value of SWP in the soil layer was reached before the peak rainfall; this occurrence was common at 60 cm (Fig. S3c), and may be due to the influence of macropores in the soil and preferential flow. The MARS model showed that the influence factors (e.g., antecedent water potential conditions, amplitude of SWP, maximum rate of SWP change, and time to maximum intensity) on the three variables had a multivariable codominant effect (Fig. 6). We also found that SWP for the shallow layers (20–40 cm) was positively correlated with other factors such as soil temperature, atmospheric temperature, and vapor pressure (P = 0.0018) (Fig. S4). Large rainfall events (> 15 mm) influence deep SWP (60 cm) and the positive correlation between SWP and soil temperature (T_s) was enhanced with the increase of rainfall treatment level (Fig. S5).

3.4 Plant Physiological Status Changes Induced by SWP Improvement

We analyzed the responses of plant physiological characteristics (photosynthetic rate, P_r; stomatal conductance, g_s; transpiration rate, T_r; water use efficiency, WUE) to different SWP dynamics under varied rainfall pulses (0–2 mm, 2–5 mm, and 5–10 mm). Small rainfall events (0–2 mm) can cause an average increase of 1.20 ± 0.81 MPa in surface SWP (20 cm) with antecedent rainfall conditions, which could promote plant physiological activity. For example, except for a few cases (-10% and + 20%), the average changes of photosynthetic rate (ΔP_r), stomatal conductance (Δg_s), and transpiration rate (ΔT_r) of HA after small rainfall events (0–2 mm) under different treatments increased, among which the photosynthetic rate (P_r) increased the most, with an average increase of 6.51 μmol CO_2 $m^{-2}s^{-1}$ under seven treatments (Table S1). However, P_r decreased after other events (2–5 mm and 5–10 mm) under increased rainfall treatments. Especially after 5–10 mm rainfall, ΔP_r dramatically decreased with the increase of rainfall magnitude (from + 10% to + 30%). The average change of water use efficiency (ΔWUE) of HA under different treatments after small rainfall events (0–2 mm) rose about 1.22 μmol CO_2·$mmol^{-1}$ H_2O (Table S1), while it was − 0.09 μmol CO_2·$mmol^{-1}$ H_2O after 5–10 mm rainfall events. In general, small rainfall events (0–2 mm) could increase physiological indices and promote the physiological activities of HA over time.

4. Discussion

4.1 SWP-Response Features and Potential Mechanisms

The response of SWP to rainfall varies with the seasons, which can be divided into three main periods: stable period (May to early June), increasing period (July to August) and fading period (September to October). Rainfall is rare and infrequent throughout the stable period. During the growth phase, soil moisture was obtained by rainfall events with high total amount and intensity. SWP increased and fluctuated frequently, with multiple peaks of water potential, concentrated in -0.01~-0.0001 MPa. The SWP declined together with the overall amount, frequency, and intensity of rainfall during the fading period. The response of SWP to rainfall events, at different depths, is a complex process, and is mainly controlled by the rainfall event size, the duration of the event, and the rainfall intensity (Heisler-White et al., 2008; Yaseef et al., 2009). The size of a rainfall event affects the value of SWP and determines how long the higher water potential value can be maintained. Therefore, rainfall regulates SWP dynamics at both long and short time scales. In the shallow soil layer (20–40 cm), large rainfall events (> 15 mm) produced a large SWP value and a long duration of the SWP response, while small events (< 5 mm) led only to weak and short-term changes of SWP. Previous studies have found similar response characteristics (Song et al., 2009). An increase in rainfall duration delays the response time of SWP; long-duration heavy rainfall events, especially, will significantly prolong the response time of SWP. Rainfall intensity mainly affects the response speed of SWP at the beginning of an event (Singh et al., 2021), and high-intensity rainfall can cause a significant shift in surface SWP (20–40 cm) in a short

period of time, but may not have an immediate impact on deep soil (60 cm). This effect may be related to the overly permeable surface runoff that occurs when instantaneous rainfall intensity is greater than instantaneous infiltration intensity (Nanda and Sen, 2021). The excess rainfall is consumed in the form of runoff rather than infiltration, resulting in less change in deep SWP.

4.2 Factors Affecting SWP Responses to Pulsed Rainfall

The response of SWP to rainfall events is mainly affected by rainfall characteristics (Heisler-White et al., 2008; Yaseef et al., 2009). Yet antecedent SWP conditions and the duration of the dry interval also affect the time, rate and threshold of SWP response processes. Studies of soil moisture have shown that small rainfall events have no obvious effect on soil moisture content (Franco and Nobel, 1990; Reynolds et al., 2004), but they have a superposition effect with large rainfall events interspersed with short drought intervals (He et al., 2012; Singh et al., 2021; Wang et al., 2013; Yu et al., 2015). Our research on SWP has found a similar "superimposed effect." Small rainfall events (< 5 mm) can cause significant changes in surface layer (20 cm) SWP—nearly 3 MPa. A very small rainfall (< 2 mm) is usually ignored in most studies, since its ecological benefits are negligible (Heisler-White et al., 2008), but they can still increase the SWP at 20-cm depth by 1.20 ± 0.81 MPa on average under the influence of antecedent rainfall. The maximum $\Delta\psi$ was nearly half (48.98%) of the antecedent SWP (one hour before the rainfall) (Table 3). This improvement in SWP is critical for desert plants in drier environments before rainfall, as these small rainfall events may keep some plants that are near the wilting point from dying.

Table 3
Comparison between the response of 20-cm SWP to new rainfall (2 mm) and antecedent SWP, under the conditions of rainfall within 48 hours before rainfall (R) and no rainfall within 168 hours before rainfall (NR)

Treatment	R$\Delta\psi$ (MPa)	NR$\Delta\psi$ (MPa)	RASWP (MPa)	NRASWP (MPa)	R$\Delta\psi$/ ASWP (%)	NR$\Delta\psi$/ ASWP (%)
-30%	0.87	0.33	-3.14	-3.60	27.84%	9.20%
-20%	0.94	0.45	-3.28	-5.09	28.56%	8.82%
-10%	2.83	1.83	-5.78	-7.91	48.98%	23.12%
CK	0.46	0.20	-2.88	-2.71	15.98%	7.56%
+ 10%	0.38	0.38	-2.4	-4.04	15.63%	9.43%
+ 20%	0.66	0.22	-3.33	-3.31	19.94%	6.58%
+ 30%	1.51	2.67	-3.46	-9.59	43.57%	27.82%

There is a delay in the reaction of SWP to rainfall, the shortest delay being between 0.3 and 2 hours (Fig. S6). Therefore, the peak SWP is usually followed by the peak rainfall (T_{p-p} is positive). It is connected to canopy rainfall interception, soil texture, soil organic matter, soil temperature, soil air migration and plant physiological activity. Water cannot enter shortly after the start of rainfall because the canopy intercepts the rainfall (Sun et al., 2021). In addition, water infiltration rates vary because of the variability of soil texture and porosity, and water potential responds differently to rainfall in various soil layers (Sun et al., 2021). Moreover, as drying times rise, soil organic matter becomes more hydrophobic, and following soaking, the increase in water potential slows down. The dynamic of SWP can also be impacted by air migration among soil particles and the limiting effect of soil temperature on the fluctuation of water potential throughout the infiltration process (Walthert and Schleppi, 2018; Wang et al., 2018). We also conjectured that in the initial stage of rainfall, a moist soil surface causes the roots of HA to absorb water, resulting in a brief drop in water potential, but this effect needs to be further confirmed. Moreover, the long response-time limitation of MPS-2 probes caused by contact with hydrophobic substances in soil may delay the sensors' ability to measure SWP and the hysteresis error thus distorts the true SWP value (Degré et al., 2017; Devices, 2016). Additional restrictions like inadequate data logger battery power, data transmission interruptions, sensor ceramic disc contamination, etc. may further impair the SWP reaction (Devices, 2016). However, it is also possible that the deep-layer SWP responds earlier than the shallow-layer SWP, and peaks earlier than the rainfall event (T_{p-p} is negative). Furthermore, the presence of soil macropores can lead rainfall to rapidly create preferential flow channels, and thus transport

water to the deeper soil, causing the peak SWP to appear early in some soil layers. Overall, the water and energy balance of the near-surface environment in dry regions is significantly influenced by the combined effect of a number of elements.

4.3 Plant Physiological Status Affected by SWP Responses: Implications for Plant Water-Use Strategies

In desert regions with inadequate water supplies, rainfall is a crucial source of water for maintaining the life of desert plants. The dynamics of SWP are impacted by changes in the geographical and temporal pattern of rainfall, which in turn influences plant physiology and ecology (Campbell and Norman, 2012). Rainfall of over 5 mm has generally been regarded as the threshold of ecologically available rainfall. However, Lauenroth and Bradford (2012) proposed that rainfall events of less than 5 mm were vital for controlling the water balance processes in arid ecosystems. We found that small rainfall events (< 5 mm) after large events can promote plant physiological activity, and even smaller events (< 2 mm) can enhance HA water use efficiency, allowing HA to survive in low SWP (about − 3.5 MPa), which is far lower than the lowest SWP value for the recently reported growth of HA (-2.82 MPa) (Yang et al., 2014b). This confirms our hypothesis that small rainfall events promote the water use and survival of desert plants. Small rainfall events (< 5 mm) perform a “superposition role” (antecedent SWP circumstances and new occurrences create a continuous sequence of events), as described by Reynolds et al. (2004) and Gemechu Legesse et al. (2021). They can help to reduce water stress, stimulate tissue healing, sustain the continuous water consumption of HA, and prevent physiological death. Additionally, Petrie et al. (2015) emphasized that small rainfall events (< 5 mm) have "legacy effects" whose reduction limits the capacity of soils to react to heavy rainfall, potentially exacerbating the negative effects of drought and impeding vegetation recovery in subsequent years of higher rainfall.

Compared with large rainfall events (> 5 mm), HA water use efficiency was significantly improved within a day after small rainfall (< 2 mm) (1.22 ± 0.74 μmol CO_2·$mmol^{-1}$ H_2O on average) (Table S1). As Reynolds et al. (2000) stressed, enormous volumes of rainfall may not convert into any net production, while small amounts of rainfall suited to the phenology of some species can result in large responses from plants. Plants' water consumption would be more efficient and conservative, the more the plants used highly unstable water sources in their environment (Ehleringer and Mooney, 1983). Small rainfall provides only an unstable supply of water for HA, due to its long-time gap, low amount, and varied intensity. HA can effectively use surface soil water through its shallow roots when SWP rises. Under future climate change with more extreme rainfall events and longer periods of drought (Chen et al., 2014; Scanlon et al., 2005), a series of small rainfall events after large events is critical. The water use trait of HA was more opportunistic than that of most plants, and HA’s utilization of small rainfall events may also be more efficient. HA might possibly make better use of other organs to improve water utilization efficiency, such as foliar water uptake (FWU) (Gong et al., 2019). However, the water potential threshold of HA is still unclear because its water supply and use mode are unknown. Hence, it is necessary to reexamine the threshold of ecologically available rainfall, which is critical for effective moisture and the survival of vegetation in water-stressed desert areas.

5. Conclusions

The response features of SWP to pulsed rainfall and the water-use strategy of HA in the desert area in northwest China were analyzed. This work has shown that SWP in desert soil is sensitive to rainfall event sizes, and has highlighted the significance of the ecological effects of small rainfall events (< 5 mm) and the non-negligible role of very small rainfall events (< 2 mm). Heavy rainfall events (> 20 mm) can maintain the SWP at a high value for a long time at a depth of 60 cm, while small rainfall events can only affect the shallow layer (20–40 cm). Very small events can also increase SWP and play a vital role in promoting plants’ use of water. Therefore, there is a need to re-examine ecologically valid rainfall thresholds.

The most important factors affecting SWP's response to rainfall are antecedent SWP, rainfall amplitude, rainfall intensity, and soil temperature. Global climate change has increased the number of heavy rainfall events, thereby increasing root-zone SWP and water storage capacity. We predict that with longer intervals between rainfall events—a condition triggered by

global climate change—surface SWP may remain low for a long time, and a series of small rainfall events after large events is critical. Small rainfall occurrences can be used more effectively by HA. The minimum SWP of HA should be redefined according to the anticipated environmental changes. The results of this study are helpful for understanding the response characteristics of SWP to rainfall and plant water-use strategies in desert areas, and provide a basis for ecological restoration in arid and semi-arid areas.

Declarations

Acknowledgments This research was jointly supported by the National Natural Science Foundation of China (42171117, 42230720), the Leading Talents Program of Gansu Province (E339040101), the Strategic Priority Research Program of the Chinese Academy of Sciences (XDA2003010102), and the 2232 International Fellowship for Outstanding Researchers Program of the Scientific and Technological Research Council of Turkey (118C329).

Funding This research was jointly supported by the National Natural Science Foundation of China (42171117, 42230720), the Leading Talents Program of Gansu Province (E339040101), the Strategic Priority Research Program of the Chinese Academy of Sciences (XDA2003010102), and the 2232 International Fellowship for Outstanding Researchers Program of the Scientific and Technological Research Council of Turkey (118C329).

Conflict of interest The authors declare that they have no conflict of interest.

Ethics approval This article does not contain any studies with human participants or animals performed by any of the authors.

Consent to participate This article does not contain any studies with human participants.

Consent for publication This article does not contain any studies with human participants.

Availability of data and materials The datasets used during the current study are available from the corresponding author on reasonable request.

Authors' contributions YYM and HL performed material preparation, data collection, and analysis. WZZ and QYY conceived and designed the experiments. YYM wrote the manuscript. YLL and JTL provided editorial advice. LG and OY commented on previous versions of the manuscript. All authors read and approved the final manuscript.

References

1. Campbell GS, Norman J (2012) An introduction to environmental biophysics. Springer Science & Business Media
2. Chen Y, Li B, Li Z, Li W (2016) Water resource formation and conversion and water security in arid region of Northwest China. J Geogr Sci 26:939-952. doi: 10.1007/s11442-016-1308-x
3. Chen Y, Wang H, Sun G (2014) Changes in extreme hydrological events. Water Resources Research in Northwest China. Springer, Berlin, Heidelberg, pp 359-404
4. Chow VT (1953) Frequency analysis of hydrologic data with special application to rainfall intensities. University of Illinois at Urbana Champaign, College of Engineering
5. Collins SL et al. (2014) A multiscale, hierarchical model of pulse dynamics in arid-land ecosystems. Annu Rev Ecol, Evol Syst 45:397-419. doi: 10.1146/annurev-ecolsys-120213-091650
6. Cui M, Caldwell MM (1997) A large ephemeral release of nitrogen upon wetting of dry soil and corresponding root responses in the field. Plant Soil 191:291-299. doi: 10.1023/A:1004290705961
7. Dasgupta P, Das BS, Sen SK (2015) Soil water potential and recoverable water stress in drought tolerant and susceptible rice varieties. Agric Water Manag 152:110-118. doi: 10.1016/j.agwat.2014.12.013

8. David TS, Gash JHC, Valente F, Pereira JS, Ferreira MI, David JS (2006) Rainfall interception by an isolated evergreen oak tree in a Mediterranean savannah. Hydrol Process 20:2713-2726. doi: 10.1002/hyp.6062
9. Dawson TE, Pate JS (1996) Seasonal water uptake and movement in root systems of Australian phraeatophytic plants of dimorphic root morphology: a stable isotope investigation. Oecologia 107:13-20. doi: 10.1007/BF00582230
10. Degré A, van der Ploeg MJ, Caldwell T, Gooren HPA (2017) Comparison of soil water potential sensors: a drying experiment. Vadose Zone J 16. doi: 10.2136/vzj2016.08.0067
11. Deo RC, Kisi O, Singh VP (2017) Drought forecasting in eastern Australia using multivariate adaptive regression spline, least square support vector machine and M5Tree model. Atmos Res 184:149-175. doi: 10.1016/j.atmosres.2016.10.004
12. Devices D (2016) MPS-2 & MPS-6 dielectric water potential sensors operator's manual. Decagon Devices, Pullman, WA
13. Dunkerley D (2008) Identifying individual rain events from pluviograph records: a review with analysis of data from an Australian dryland site. Hydrol Process 22:5024-5036. doi: 10.1002/hyp.7122
14. Ehleringer J, Mooney HA (1983) Productivity of desert and Mediterranean-climate plants. In: Lange OL, Nobel PS, Osmond CB, Ziegler H (eds) Physiological plant ecology IV: ecosystem processes: mineral cycling, productivity and man's influence. Springer Berlin Heidelberg, Berlin, Heidelberg, pp 205-231
15. Fauer FS, Ulrich J, Jurado OE, Rust HW (2021) Flexible and consistent quantile estimation for intensity-duration-frequency curves. Hydrol Earth Syst Sci 25:6479-6494. doi: 10.5194/hess-25-6479-2021
16. Franco AC, Nobel PS (1990) Influences of root distribution and growth on predicted water uptake and interspecific competition. Oecologia 82:151-157. doi: 10.1007/BF00323528
17. Friedman JH (1991) Multivariate adaptive regression splines. Ann Stat 19:1-67. doi: 10.1214/aos/1176347963
18. Gao H et al. (2020) *HaASR1* gene cloned from a desert shrub, *Haloxylon ammodendron*, confers drought tolerance in transgenic *Arabidopsis thaliana*. Environ Exp Bot 180. doi: 10.1016/j.envexpbot.2020.104251
19. Gemechu Legesse T et al. (2021) Small precipitation events enhance the Eurasian grassland carbon sink. Ecol Indic 131. doi: 10.1016/j.ecolind.2021.108242
20. Gong XW, Lu GH, He XM, Sarkar B, Yang XD (2019) High air humidity causes atmospheric water absorption via assimilating branches in the deep-rooted tree *Haloxylon ammodendron* in an arid desert region of Northwest China. Front Plant Sci 10:573. doi: 10.3389/fpls.2019.00573
21. Goodwell AE, Kumar P, Fellows AW, Flerchinger GN (2018) Dynamic process connectivity explains ecohydrologic responses to rainfall pulses and drought. Proc Natl Acad Sci U S A 115:E8604-E8613. doi: 10.1073/pnas.1800236115
22. Graham CB, Lin HS (2011) Controls and frequency of preferential flow occurrence: a 175-event analysis. Vadose Zone J 10:816-831. doi: 10.2136/vzj2010.0119
23. Grunzweig JM et al. (2022) Dryland mechanisms could widely control ecosystem functioning in a drier and warmer world. Nat Ecol Evol 6:1064-1076. doi: 10.1038/s41559-022-01779-y
24. Hao YB, Kang XM, Cui XY, Ding K, Wang YF, Zhou XQ (2012) Verification of a threshold concept of ecologically effective precipitation pulse: from plant individuals to ecosystem. Ecol Inform 12:23-30. doi: 10.1016/j.ecoinf.2012.07.006
25. He Z, Zhao W, Liu H, Chang X (2012) The response of soil moisture to rainfall event size in subalpine grassland and meadows in a semi-arid mountain range: a case study in northwestern China's Qilian Mountains. J Hydrol 420-421:183-190. doi: 10.1016/j.jhydrol.2011.11.056
26. Heisler-White JL, Knapp AK, Kelly EF (2008) Increasing precipitation event size increases aboveground net primary productivity in a semi-arid grassland. Oecologia 158:129-140. doi: 10.1007/s00442-008-1116-9
27. Huber K, Vanderborght J, Javaux M, Schröder N, Dodd IC, Vereecken H (2014) Modelling the impact of heterogeneous rootzone water distribution on the regulation of transpiration by hormone transport and/or hydraulic pressures. Plant Soil 384:93-112. doi: 10.1007/s11104-014-2188-4
28. Hudson SA (2019) Soil water potential response to double funneling of recipitation on a forested, Mid-Atlantic hillslope. University of Delaware

29. Huxman TE et al. (2004) Precipitation pulses and carbon fluxes in semiarid and arid ecosystems. Oecologia 141:254-268. doi: 10.1007/s00442-004-1682-4
30. Lauenroth WK, Bradford JB (2012) Ecohydrology of dry regions of the United States: water balance consequences of small precipitation events. Ecohydrology 5:46-53. doi: 10.1002/eco.195
31. Li-Cor I (2011) Using the Li-6400/Li-6400XT portable photosynthesis system.
32. Liu H et al. (2020) Modeling the physiological responses of a desert shrub to rainfall pulses in an arid environment in northwestern China. J Arid Environ 183. doi: 10.1016/j.jaridenv.2020.104277
33. Long RW, D'Antonio CM, Dudley TL, Hultine KR (2021) Variation in salinity tolerance and water use strategies in an introduced woody halophyte (*Tamarix* spp.). J Ecol 109:3807-3817. doi: https://doi.org/10.1111/1365-2745.13758
34. Lozano-Parra J, van Schaik NLMB, Schnabel S, Gómez-Gutiérrez Á (2016) Soil moisture dynamics at high temporal resolution in a semiarid Mediterranean watershed with scattered tree cover. Hydrol Process 30:1155-1170. doi: 10.1002/hyp.10694
35. Luo S, Lu N, Zhang C, Likos W (2022) Soil water potential: a historical perspective and recent breakthroughs. Vadose Zone J 21. doi: 10.1002/vzj2.20203
36. McKenzie N, Coughlan K, Cresswell H (2002) Soil physical measurement and interpretation for land evaluation. CSIRO publishing, Melbourne, Australia
37. Nanda A, Sen S (2021) A complex network theory based approach to better understand the infiltration-excess runoff generation thresholds. J Hydrol 603:127038. doi: 10.1016/j.jhydrol.2021.127038
38. Nolz R, Kammerer G, Cepuder P (2013) Calibrating soil water potential sensors integrated into a wireless monitoring network. Agric Water Manag 116:12-20. doi: 10.1016/j.agwat.2012.10.002
39. Novick KA et al. (2022) Confronting the water potential information gap. Nat Geosci 15:158-164. doi: 10.1038/s41561-022-00909-2
40. Noy-Meir I (1973) Desert ecosystems: environment and producers. Annu Rev Ecol Syst 4:25-51
41. Ogle K, Reynolds JF (2004) Plant responses to precipitation in desert ecosystems: integrating functional types, pulses, thresholds, and delays. Oecologia 141:282-294. doi: 10.1007/s00442-004-1507-5
42. Papendick RI, Campbell GS (1981) Theory and measurement of water potential. In: Parr JF, Gardner WR, Elliott LF (eds) Water potential relations in soil microbiology, vol 9. Soil Science Society of America, Madison, WI, USA, pp 1-22
43. Passioura JB (1982) Water in the soil-plant-atmosphere continuum. In: Lange OL, Nobel PS, Osmond CB, Ziegler H (eds) Physiological plant ecology II: water relations and carbon assimilation, vol 12. Springer, Berlin, Germany, pp 5-33
44. Petrie MD, Collins SL, Litvak ME (2015) The ecological role of small rainfall events in a desert grassland. Ecohydrology 8:1614-1622. doi: 10.1002/eco.1614
45. Polley HW, Collins HP, Reichmann LG, Fay PA (2016) CO_2 and soil water potential as regulators of the growth and N fraction derived from fixation of a legume in tallgrass prairie communities. Plant Soil 409:361-370. doi: 10.1007/s11104-016-2971-5
46. Potts DL, Huxman TE, Enquist BJ, Weltzin JF, Williams DG (2006) Resilience and resistance of ecosystem functional response to a precipitation pulse in a semi-arid grassland. J Ecol:23-30. doi: 10.1111/j.1365-2745.2005.01060.x
47. Prăvălie R (2016) Drylands extent and environmental issues. A global approach. Earth-Sci Rev 161:259-278. doi: 10.1016/j.earscirev.2016.08.003
48. Reynolds JF, Kemp PR, Ogle K, Fernandez RJ (2004) Modifying the 'pulse-reserve' paradigm for deserts of North America: precipitation pulses, soil water, and plant responses. Oecologia 141:194-210. doi: 10.1007/s00442-004-1524-4
49. Reynolds JF, Kemp PR, Tenhunen JD (2000) Effects of long-term rainfall variability on evapotranspiration and soil water distribution in the Chihuahuan Desert: a modeling analysis. Plant Ecol 150:145-159. doi: 10.1023/A:1026530522612
50. Rodriguez-Iturbe I (2000) Ecohydrology: a hydrologic perspective of climate-soil-vegetation dynamies. Water Resour Res 36:3-9. doi: 10.1029/1999wr900210

51. Sala OE, Lauenroth W (1982) Small rainfall events: an ecological role in semiarid regions. Oecologia 53:301-304. doi: 10.1007/BF00389004
52. Scanlon BR, Levitt DG, Reedy RC, Keese KE, Sully MJ (2005) Ecological controls on water-cycle response to climate variability in deserts. Proc Natl Acad Sci U S A 102:6033-6038. doi: doi:10.1073/pnas.0408571102
53. Schimel DS (2010) Drylands in the earth system. Science 327:418-419. doi: 10.1126/science.1184946
54. Schwinning S, Sala OE (2004) Hierarchy of responses to resource pulses in arid and semi-arid ecosystems. Oecologia 141:211-220. doi: 10.1007/s00442-004-1520-8
55. Schwinning S, Starr BI, Ehleringer JR (2003) Dominant cold desert plants do not partition warm season precipitation by event size. Oecologia 136:252-260. doi: 10.1007/s00442-003-1255-y
56. Shan L et al. (2009) Influence of moisture on the growth and biomass allocation in *Haloxylon ammodendron* and *Tamarix ramosissima* seedlings in the shelterbelt along the Tarim Desert Highway, Xinjiang, China. Sci Bull 53:93-101. doi: 10.1007/s11434-008-6010-7
57. Singh NK, Emanuel RE, McGlynn BL, Miniat CF (2021) Soil Moisture Responses to Rainfall: Implications for Runoff Generation. Water Resour Res 57:e2020WR02882. doi: 10.1029/2020wr028827
58. Song X, Wang S, Xiao G, Wang Z, Liu X, Wang P (2009) A study of soil water movement combining soil water potential with stable isotopes at two sites of shallow groundwater areas in the North China Plain. Hydrol Process 23:1376-1388. doi: 10.1002/hyp.7267
59. Sun F, Xiao B, Li S, Kidron GJ (2021) Towards moss biocrust effects on surface soil water holding capacity: soil water retention curve analysis and modeling. Geoderma 399:115120. doi: 10.1016/j.geoderma.2021.115120
60. Ulrich J, Jurado OE, Peter M, Scheibel M, Rust HW (2020) Estimating IDF curves consistently over durations with spatial covariates. Water 12. doi: 10.3390/w12113119
61. Walthert L, Schleppi P (2018) Equations to compensate for the temperature effect on readings from dielectric Decagon MPS-2 and MPS-6 water potential sensors in soils. J Plant Nutr Soil Sci 181:749-759. doi: 10.1002/jpln.201700620
62. Wang C, Fu B, Zhang L, Xu Z (2018) Soil moisture-plant interactions: an ecohydrological review. J Soils Sed 19:1-9. doi: 10.1007/s11368-018-2167-0
63. Wang S, Fu B, Gao G, Liu Y, Zhou J (2013) Responses of soil moisture in different land cover types to rainfall events in a re-vegetation catchment area of the Loess Plateau, China. Catena 101:122-128. doi: 10.1016/j.catena.2012.10.006
64. Yang LH, Bastow JL, Spence KO, Wright AN (2008) What can we learn from resource pulses. Ecology 89:621-634. doi: 10.1890/07-0175.1
65. Yang Q, Zhao W, Liu B, Liu H (2014a) Physiological responses of *Haloxylon ammodendron* to rainfall pulses in temperate desert regions, Northwestern China. Trees 28:709-722. doi: 10.1007/s00468-014-0983-4
66. Yang W, Feng W, Jia Z, Zhu Y, Guo J (2014b) Soil water threshold for the growth of *Haloxylon ammodendron* in the Ulan Buh desert in arid northwest China. S Afr J Bot 92:53-58. doi: 10.1016/j.sajb.2014.02.001
67. Yaseef NR, Yakir D, Rotenberg E, Schiller G, Cohen S (2009) Ecohydrology of a semi-arid forest: partitioning among water balance components and its implications for predicted precipitation changes. Ecohydrology 3:143-154. doi: 10.1002/eco.65
68. Yu W, Xin-jun Z, Yan L (2013) Photosynthetic responses of different plant functional types to small rainfall events in a non-disturbed desert. Chin J Ecol 32:2591-2597
69. Yu Y et al. (2015) Responses of vertical soil moisture to rainfall pulses and land uses in a typical loess hilly area, China. Solid Earth 6:595-608. doi: 10.5194/se-6-595-2015
70. Zhao W, Chang X, Zhang Z (2009) Transpiration of a Linze jujube orchard in an arid region of China. Hydrol Process 23:1461-1470. doi: 10.1002/hyp.7272
71. Zhao W, Liu B (2010) The response of sap flow in shrubs to rainfall pulses in the desert region of China. Agric For Meteorol 150:1297-1306. doi: 10.1016/j.agrformet.2010.05.012

72. Zheng C, Wang Q (2014) Water-use response to climate factors at whole tree and branch scale for a dominant desert species in central Asia: *Haloxylon ammodendron*. Ecohydrology 7:56-63. doi: 10.1002/eco.1321

73. Zheng C, Wang Q (2015) Seasonal and annual variation in transpiration of a dominant desert species, *Haloxylon ammodendron*, in Central Asia up-scaled from sap flow measurement. Ecohydrology 8:948-960. doi: 10.1002/eco.1547

74. Zou T, Li Y, Xu H, Xu G (2009) Responses to precipitation treatment for *Haloxylon ammodendron* growing on contrasting textured soils. Ecol Res 25:185-194. doi: 10.1007/s11284-009-0642-1

Figures

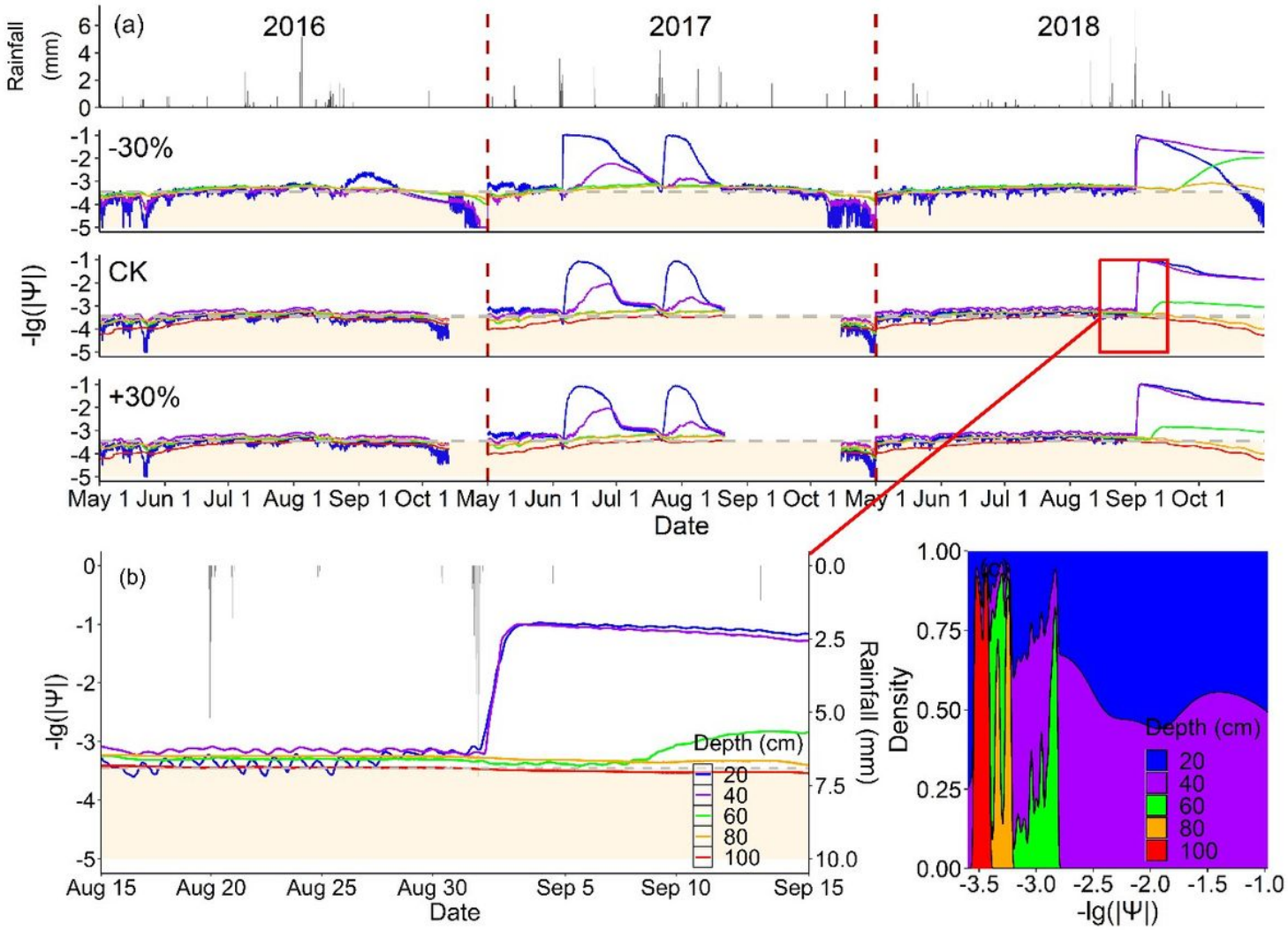


Figure 1

(a) Daily rainfall and corresponding daily soil water potential (SWP) changes at five soil depths (20, 40, 60, 80 and 100 cm) under different rainfall interception treatments (-30%, CK, and +30%) from May 1 to October 31, 2016 to 2018; (b) SWP response from August 15 to September 15, 2018; and (c) corresponding SWP density at different depths. The gray dotted line indicates the minimum SWP for *Haloxylon ammodendron* (HA) growth according to Yang et al. (2014b)

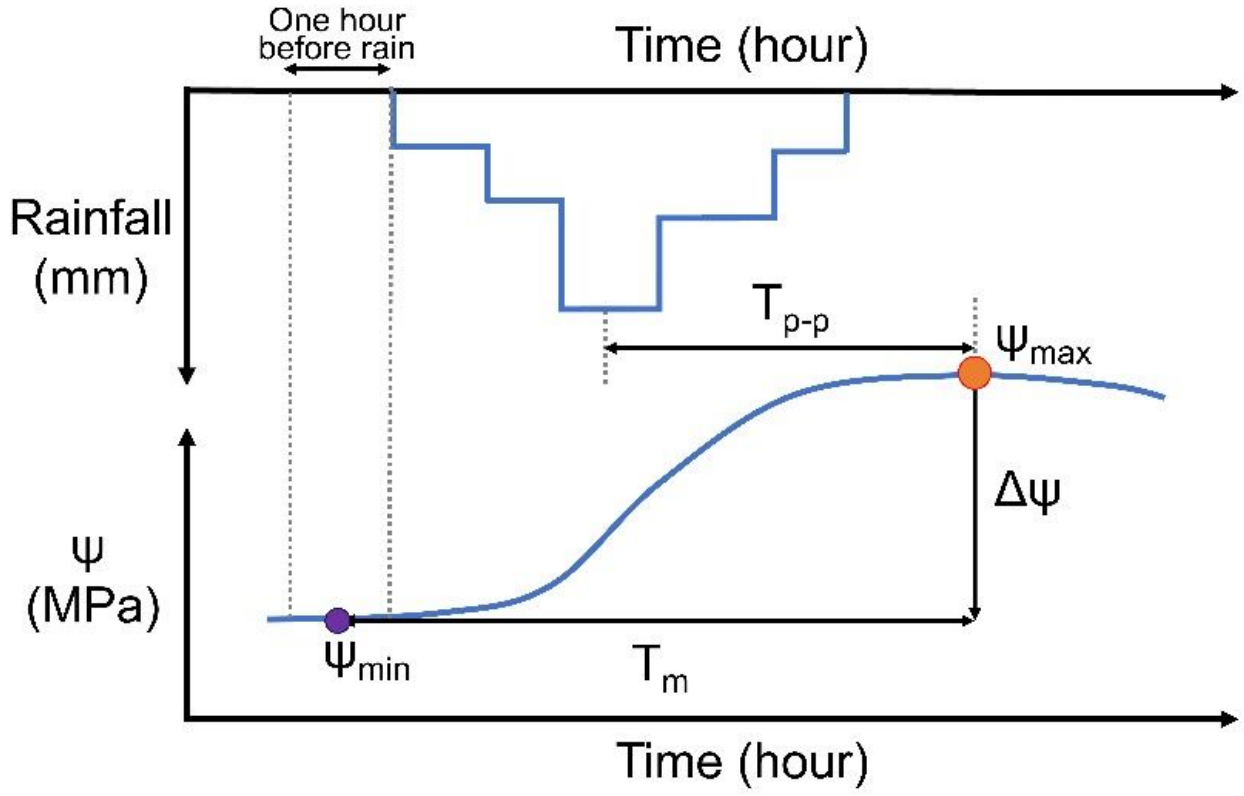


Figure 2

SWP dynamics changes during rainfall. Adapted from Singh et al. (2021)

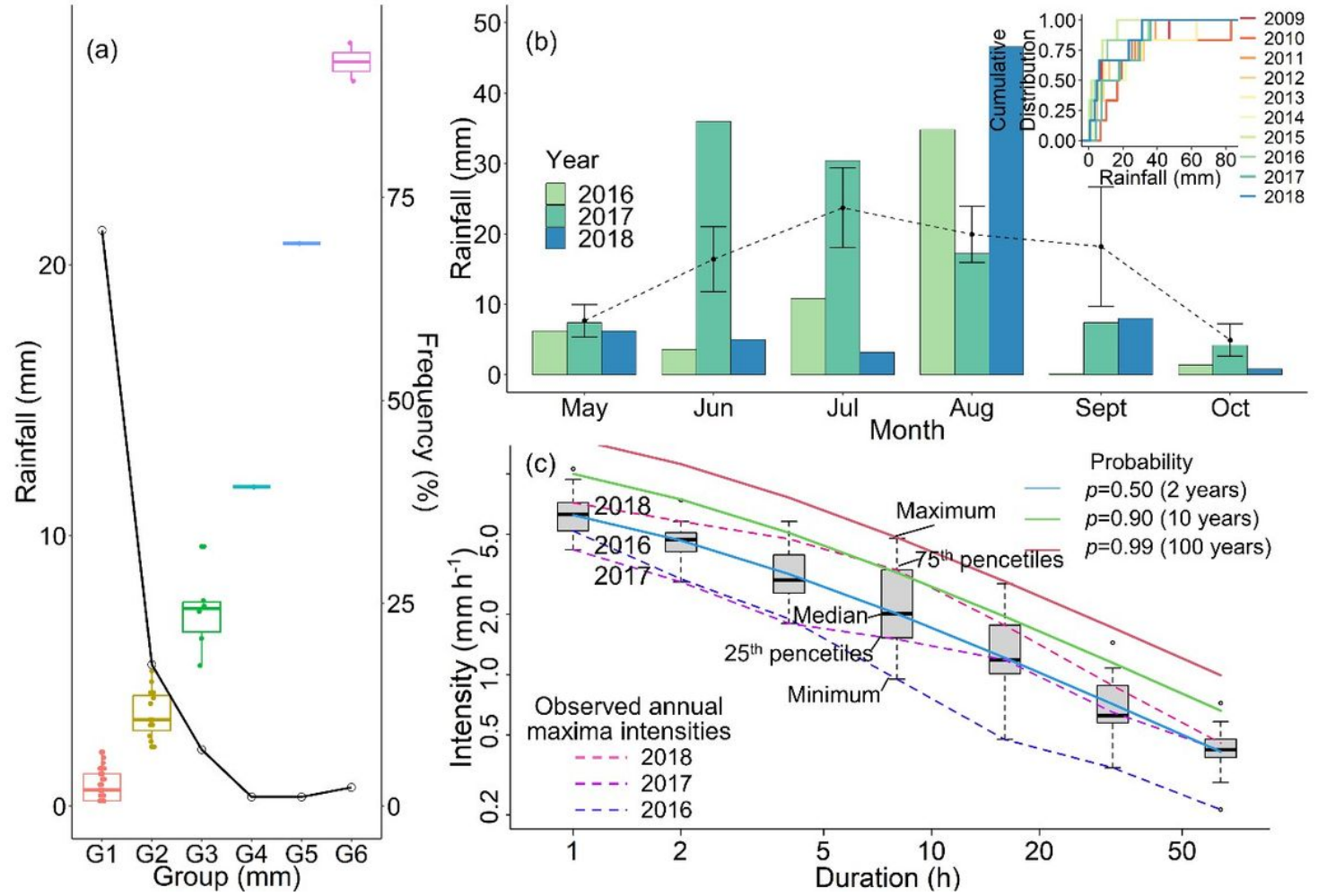


Figure 3

Rainfall distribution characteristics of the study area. (a) Rainfall distribution (mean ± SD) and frequency of occurrence (black line) in different groups (G1 to G6 represent 0-2, 2-5, 5-10, 10-15, 15-20, and 20-30 mm rainfall groups, respectively) from 2016 to 2018; (b) rainfall distribution in different months (the black dotted line represents the multi-year average from 2009 to 2018, mean ± SD) and annual cumulative rainfall from 2009 to 2018; (c) IDF curve estimate using rainfall data from 2009 to 2018 for the study area. The distributions of the observed annual maximum intensities are shown as box-and-whisker plots and the dotted line represents the observed annual maximum intensities from 2016 to 2018

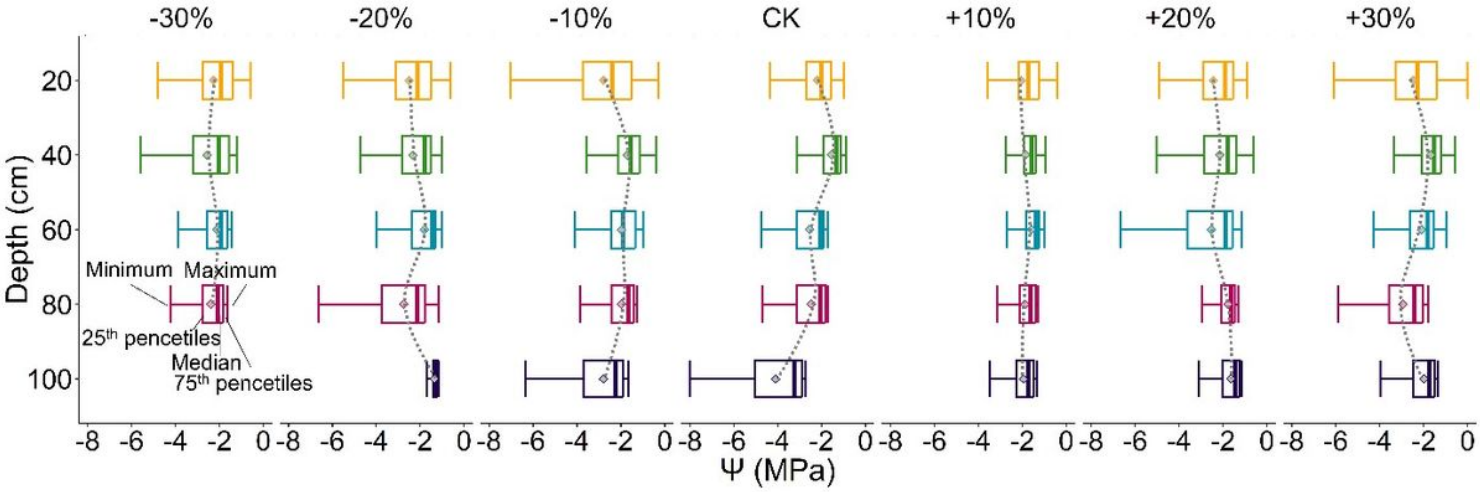


Figure 4

Vertical changes in SWP (mean ± SD) at five soil depths under six rainfall interception treatments during the study period (relative outliers removed). The upper and lower quartiles of the rectangles represent the upper and lower quartiles respectively, and the horizontal lines inside the rectangles represent the medians. The gray diamonds show the mean values

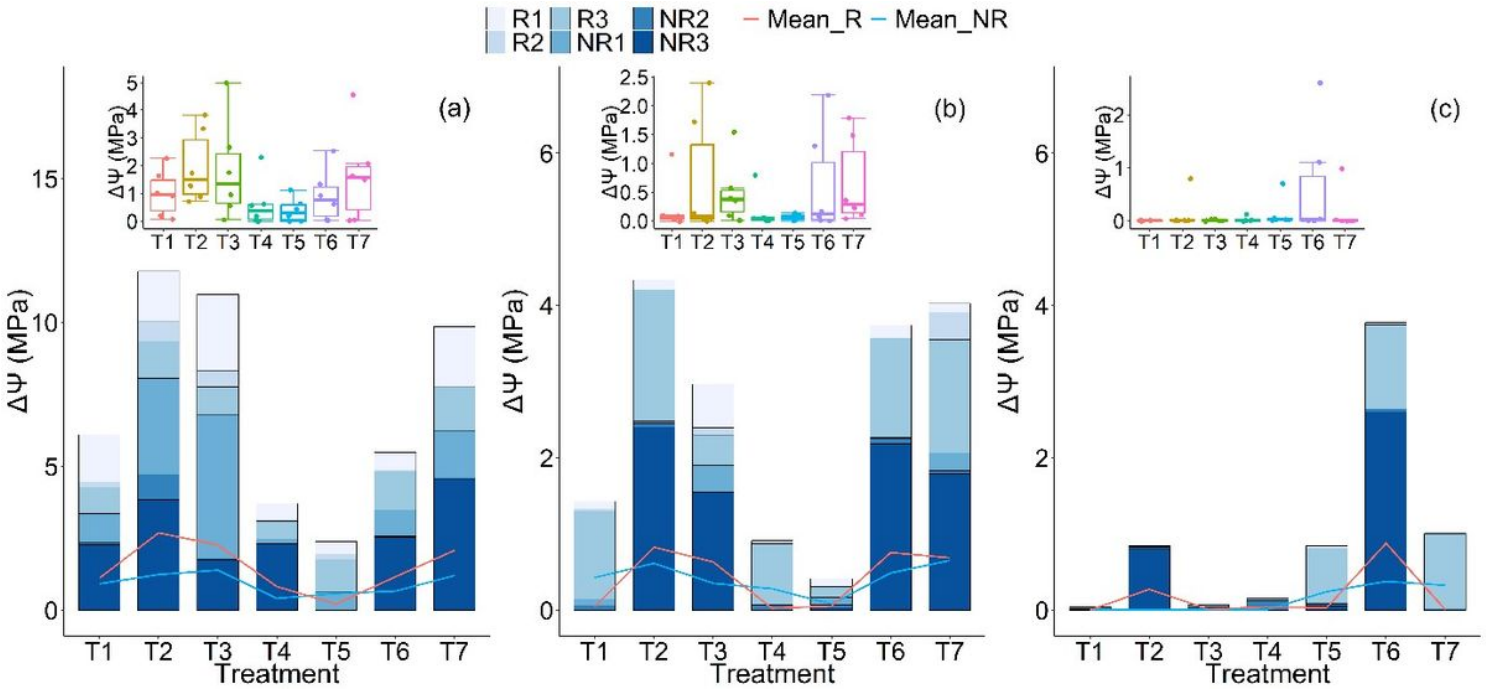


Figure 5

Response values of SWP (mean ± SD)at three soil depths (a, 20 cm; b, 40 cm; c, 60 cm) under different treatments for two different antecedent rainfall conditions: events with rainfall in the first 48 hours (R) and with no rainfall for 168 hours or more (NR). T1 to T7 represent -30%, -20%, -10%, CK, +10%, +20%, and +30% rainfall treatments, respectively. Numbers 1-3 represent three rainfall groups: 0-5 mm, 5-15 mm, and > 15 mm, respectively. Red line, average increase of SWP with antecedent rainfall; blue line, average increase in SWP without antecedent rainfall

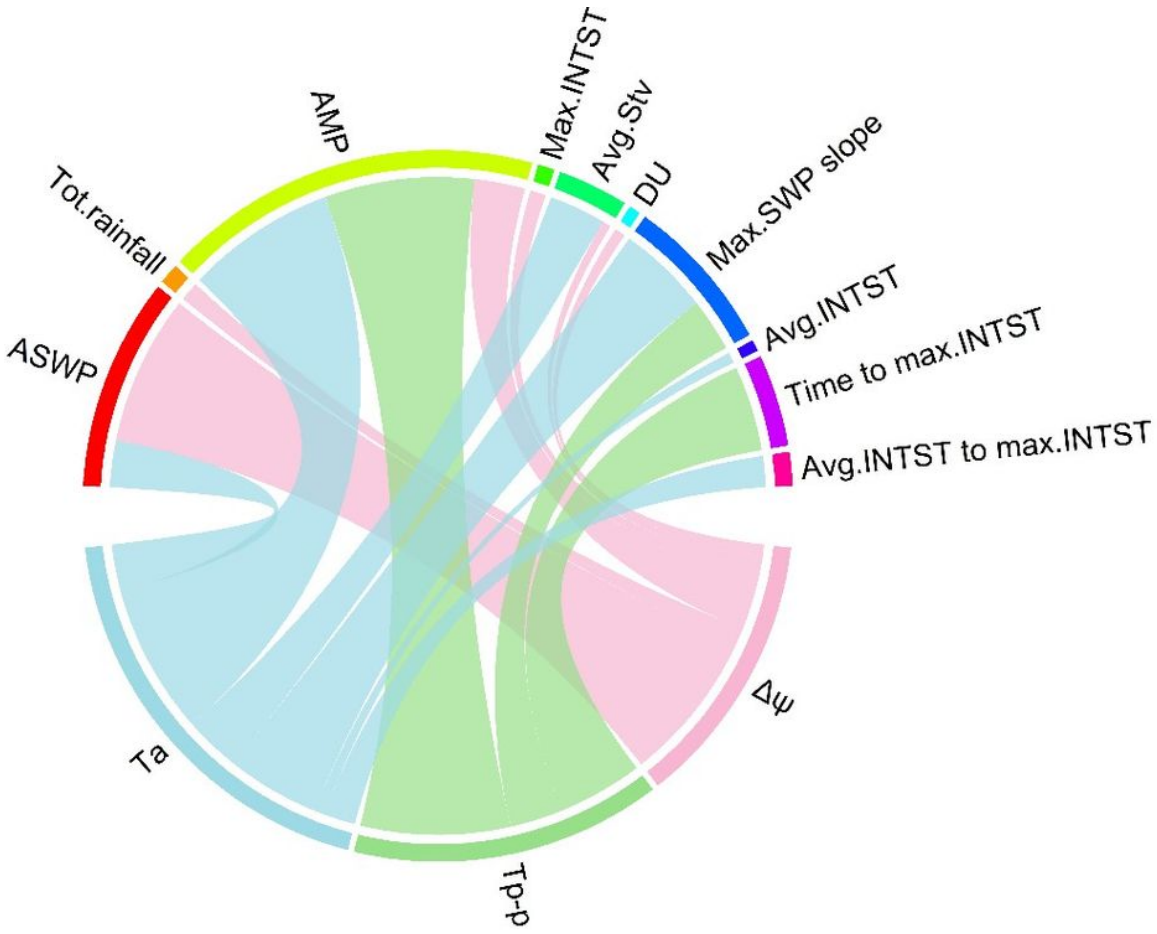


Figure 6

Relative importance of the influential variables of $\Delta\psi$ (pink link), T_a (blue link), and $T_{p\text{-}p}$ (green link) derived from the MARS model. ASWP, antecedent SWP (soil water potential value one hour before rainfall); Tot. rainfall, total amount of rain; AMP, amplitude of SWP; Max. INTST, maximum rainfall intensity; Avg. Stv, average hourly rate of change in soil temperature; DU, duration of rainfall; Max. SWP slope, maximum slope of SWP change; Avg. INTST, average rainfall intensity; Time to max. INTST, time to maximum rainfall intensity; Avg. INTST to max. INTST, average intensity from the start to the time of maximum intensity

Supplementary Files

This is a list of supplementary files associated with this preprint. Click to download.

- SupplementaryMaterialplaintext.docx